

Oscillatory effect of a magnetic field on the rate of a chemical reaction

G. S. Krinchik and R. A. Shvartsman

Moscow State University

(Submitted July 11, 1974)

Zh. Eksp. Teor. Fiz. 67, 2326-2334 (December 1974)

The oscillatory dependences of the nickel carbonylation reaction rate are investigated at various orientation of the magnetic field in the (001) plane and on increase of the temperature to 100°C. At $H \parallel [100]$ a pure sinusoidal oscillation of the reaction rate with a period of $\Delta H = 40$ Oe is observed, and the reaction rate is changed by a factor of six. At $H \parallel [110]$, cases are observed when a change of the field strength by 1% and of the induction by 0.1% results in a 40-fold change of the reaction rate. A hole pocket at the X point of nickel is chosen such that quantization of its extremal cross section agrees qualitatively with the observed oscillations of the reaction rate with respect to their period, anisotropy, and temperature dependence.

An oscillatory change in the rate of the heterogeneous chemical reaction of the carbonylation of nickel in a magnetic field was observed earlier^[1], and it was suggested that the observed oscillations are due to quantization of the electron energy spectrum of the nickel in the magnetic field. We present below new results of an experimental study of this effect, using an improved measurement procedure, and consider also certain possibilities of its explanation, based on modern notions concerning the electronic structure of paramagnetic nickel.

A schematic diagram of the experimental setup is shown in Fig. 1. The magnetic-field source was an electromagnet having 15×15 cm pole pieces and a gap of 5 cm. With this geometry, a homogeneous magnetic field was produced in the central part of the gap, with a gradient not larger than 0.5 Oe/cm. The electromagnet winding was fed from NKN-500 storage batteries, the direct current was registered by measuring the voltage across a standard 0.1 Ω resistor with an R-304 potentiometer and a M-95 indicating microammeter. The current was regulated with a set of R-326 resistors connected to form a rheostat. The stability of the magnetic field was ± 1 Oe.

The chemical part of the setup consisted of the system used to produce and purify the CO gas, a reactor for the carbonylation, and a system for analyzing the end products of the reaction. The procedure used to obtain the carbon monoxide should provide a reaction gas of high purity. The reason for the more stringent requirements on its purity is that slight oxygen impurities in the carbon monoxide passivate completely the carbonylation process when the reaction is carried out at normal pressure and at room temperature. The carbon monoxide was obtained and subsequently purified by well-known methods^[2]. The reaction gas was obtained by the action of formic acid on sulfuric acid heated in a water bath to 80°C. The released carbon monoxide was fed to the purification system and then to the reactor. The purification system provided for the removal of oxygen, water vapor, and CO₂ from the CO. To absorb the carbon dioxide, the obtained gas was passed through dry and liquid lye. The oxygen was removed in two stages: first, copper chips previously reduced in a hydrogen stream first removed the O₂ from the carbon monoxide, and then the traces of the oxygen were removed by passing the reaction gas through active copper in silica gel.

The procedure for preparing the active copper was the following: 120 g of CuCO₃ · Cu(OH)₂ was dissolved

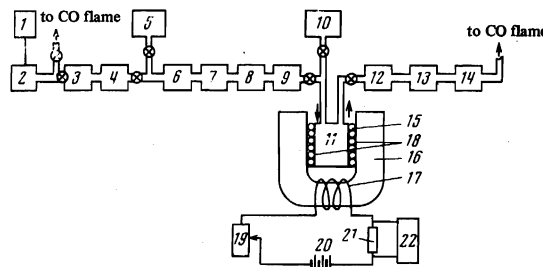


FIG. 1. Schematic diagram of setup: 1—formic acid, 2—sulfuric acid, 3—50% solution of KOH, 4—dry KOH lye, 5—bottle with hydrogen, 6—copper chips, 7—active copper, 8—calcium chloride, 9—P₂O₅, 10—bottle with helium, 11—reactor, 12—absorber system, 13—gas meter, 14—rheometer, 15—electric oven, 16—electromagnet, 17—electromagnet winding, 18—thermal insulation, 19—set of R-326 resistors, 20—NKN-500 storage batteries, 21—0.1- Ω standard resistor, 22—R-304 potentiometer.

in two liters of concentrated ammonia solution. The solution was then evaporated dry with 420 g of purified silica gel. The obtained mass was rolled into spheres of diameter up to 5 mm and dried at 150–180°C. After reducing in a hydrogen stream at 300–350°C, the active copper assumed a brownish-violet color, thus indicating that the compound was ready for use. The spheres were placed in glass columns for which external heating was provided. The working temperature of the active copper in silica gel was 220°C. The preliminary and final purification reduced the oxygen content in the CO to 10⁻⁴%.

The removal of the moisture vapor from the reaction gas was with calcium chloride and phosphorus pentoxide (P₂O₅), which was mixed with asbestos fiber, dried, and then placed in a U-shaped vessel with ground-glass stoppers. The remaining moisture in the gas was 10⁻⁵%.

The carbon monoxide free of carbon dioxide and of acid and water vapor was applied to the surface of a nickel sample, which was securely mounted in the reactor. The reactor was a cylinder of 5 cm diameter and 3 cm height, made of nonmagnetic material and provided with fittings and proper valves for the entry and exit of the gas. Inside of the reactor, a socket was milled so shaped that the nickel sample fitted tightly in it and the (100) working surface was oriented parallel to the base of the reactor. A cover was screwed on the top of the reactor and tubes for the entry and exit of the gas were welded to the cover. The nickel sample was placed in the reactor socket. To secure the sample and to insulate completely the non-working surfaces of the crystal from the reaction gas, liquid glass was poured into the gaps. The reactor was sealed on top with the aid of a screw cover and a copper gasket. The gasket thickness

was chosen such that a gap of 0.2–0.5 mm remained between the working surface of the nickel single crystal and the upper cover after tightening the cover. On the outside of the reactor was placed an electric oven to heat the entire system to the specified temperature. The temperature was monitored with a thermocouple, the junction of which entered a specially provided well in the housing of the reactor. The entire system was provided with reliable thermal insulation. The employed construction of the reactor and the method of securing the sample have made it possible to reduce the single crystal directly in the reactor when heated to 400°C. In addition, the dead space over the sample was decreased to a minimum. The rate of flow of the carbon monoxide and the amount of gas passing through the system was monitored with a rheometer and with a gas meter.

The nickel carbonyl produced by the passing stream of carbon monoxide was transported out of the reactor into a system of absorbers filled with 10% solution of iodine in carbon tetrachloride. The carbonyl molecules were decomposed there, the nickel was accumulated in the absorber solution, and the released CO molecules were carried farther by the gas stream and ignited.

After 3–5 min passage of the carbon monoxide, the absorber solution was analyzed for the nickel content^[3]. The chemical analysis was based on the decomposition of the carbonyl by the iodine with release of nickel, which interacted with dimethyl glyoxyl in the presence of an oxidizer to form compounds of red color. An FÉK-56 colorimeter-nephelometer was used to determine the color intensity of the solutions, and the nickel content in micrograms was determined from a calibration curve obtained with prepared standard solutions of nickel. The described analysis is simple to perform, well worked-out, and has a high resolution, $\pm 1 \mu\text{g}$ of Ni, so that the error in the measurement of the reaction rate did not exceed $\pm 0.2 \mu\text{g}/\text{cm}^2\text{min}$.

The sample was a plate of irregular shape, cut from the single crystal in such a way that the reaction surface of 3 cm^2 area was parallel to the (110) plane (the positioning accuracy was $\pm 2^\circ$). A rotating device made it possible to orient the nickel crystal in such a way that the magnetic field was directed in the (100) plane at different angles to the crystallographic axes (accuracy $\pm 3^\circ$). In the pauses between the measurements of the individual points, helium was blown through the entire system to wash out the carbonyl from the possible stagnant zones of the reactor.

Figures 2 and 3 show the experimental plots of the reaction rate against the magnetic field intensity, obtained at room temperature and at different orientations of H relative to the crystallographic axes in the (001) plane. By way of estimate, we can indicate that a reaction rate of $1 \mu\text{g}/\text{cm}^2\text{min}$ means that one out of 100 nickel surface atoms is carried away by the carbonyl molecules per second.

Before discussing the results as a whole, we wish to make the following remarks. First, the main results of the preceding study^[1], the existence of sharply pronounced oscillations of the reaction rate of nickel carbonylation in a magnetic field, is confirmed. Also confirmed is the conclusion that low-frequency oscillations (with a period ΔH on the order of 40 Oe) appear at $H \parallel [100]$ and that high frequency oscillations ($\Delta H \sim 15$ Oe) appear at $H \parallel [110]$. It turns out here that in a physical sense we are dealing with a harmonic that is of the

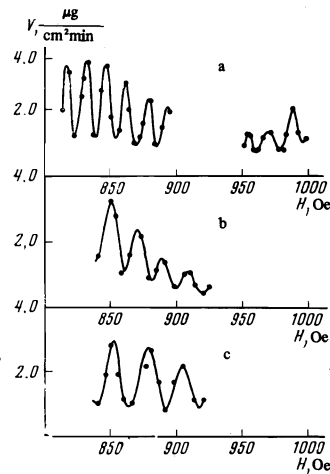


FIG. 2

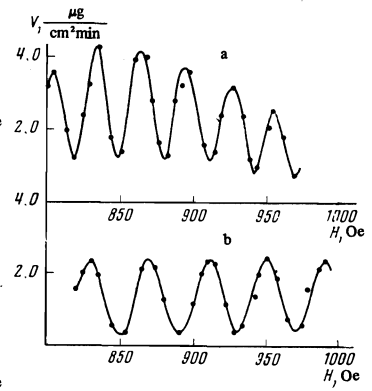


FIG. 3

FIG. 2. Nickel carbonylation reaction rate vs. the orientation of the magnetic field in the (001) plane. α is the angle between H and the [110] axis, $T = 20^\circ\text{C}$. a) $H \parallel [110]$, $\alpha = 0^\circ$; b) $\alpha = 15^\circ$; c) $\alpha = 21^\circ$.

FIG. 3. The same as in Fig. 2. a) $\alpha = 30^\circ$, b) $H \parallel [100]$, $\alpha = 45^\circ$.

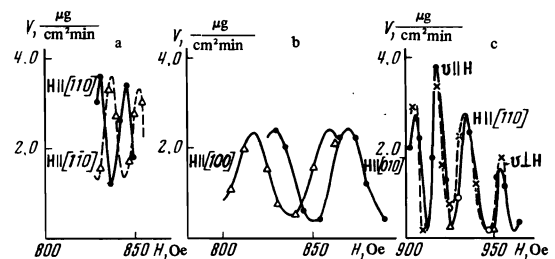


FIG. 4. a) Dependence of the reaction rate on the field at an orientation of H along two equivalent axes, [110] and $\bar{1}\bar{1}0$, in the (001) plane; b) the same for the axes [100] and $\bar{1}0\bar{1}$; c) dependence of the reaction rate V on the direction of the CO gas stream v along and across the magnetic field.

same origin, for when α is varied we observe a continuous transition of the low-frequency oscillations into high-frequency oscillations, the change in the period ΔH amounting to approximately 0.5 Oe/deg ($\Delta H = 40, 30, 26, 20,$ and 16 Oe at $\alpha = 45^\circ, 30^\circ, 21^\circ, 15^\circ,$ and 0° , respectively).

Attention is called to the perfect waveform of the oscillation curve at $H \parallel [100]$. All the experimental points fit well on a sinusoid with a period $\Delta H = 40$ Oe. The minimum and maximum values of the rate are 0.4 and $2.4 \mu\text{g}/\text{cm}^2\text{min}$; thus, the reaction rate changes by a factor of 6, in contrast to the twofold change observed earlier^[1]. One can expect that further improvement of the measurement procedure and of the preparation of the sample surface, as well as a decrease in the inhomogeneity of the magnetic field and in the inhomogeneity of the sample magnetization, will all increase the difference between the minimal and maximal values of the reaction rate, mainly of course via decreasing the minimal values.

To monitor the influence of the sample shape on the results, and in particular on the anisotropy of the effect, measurements were performed with the reactor rotated 90° , i.e., with the field directed along the equivalent axes [100] and $\bar{1}0\bar{1}$, and also [110] and $\bar{1}\bar{1}0$. The results of these measurements, shown in Figs. 4a. and 4b, indicate that although the entire curve is shifted along the H axis,

the main characteristics, namely the amplitude and the period of the oscillations, remain unchanged. Figure 4c shows that the change of the direction of the CO gas stream relative to the magnetic field (the reactor cover was rotated 90°) has practically no effect on the experimental curves.

A change in the angle α leads not only to a change in the period ΔH , but also to a qualitative change in the shape of the oscillation curves. It can be concluded that when the field H deviates from the $[100]$ axis (at $\alpha \neq \pi/4$), at least two harmonics with different periods ΔH become superimposed. An asymmetry of the oscillation curves relative to the horizontal axis parallel to the H axis is observed in this case. This circumstance, which in our opinion is natural, is connected with the large amplitude of the oscillations and with the nonphysical character of the negative values of the reaction rate V , and leads to the following difficulty in the interpretation of the results: Practically each compound curve of Figs. 2 and 3, with $\alpha \neq \pi/4$, can be interpreted in two ways, either as the result of modulation of the oscillatory curve with $\Delta H \sim 20$ Oe by oscillations of much lower frequency ($\Delta H > 100$ Oe), or else as a result of beats produced by addition of two oscillations that are relatively close in frequency, with periods $\Delta H \pm \delta H$. Thus, for example, the modulation interpretation of the $V(H)$ curve, at $H \parallel [110]$, yields $\Delta H_1 = 16$ Oe and $\Delta H_2 \cong 200$ Oe, whereas the beat hypothesis yields $\Delta H_1 \cong 15$ Oe and $\Delta H_2 \cong 17$ Oe.

A more thorough study of the compound $V(H)$ oscillation curve at $H \parallel [110]$ was made at increased temperature. This was brought about by the difficulty in the measurement, which led to the desire of performing primarily experiments that yield a maximum of information, particularly temperature measurements. Measuring the temperature dependence of the carbonylation rate of polycrystalline nickel, Goldberger^[4] observed a maximum of V at $T_0 = 75^\circ\text{C}$. Measurements with our single crystal at $H = 0$ have confirmed this result (see Fig. 5). Figure 6 shows the oscillation curves obtained at different temperatures in the vicinity of T_0 . We call attention first to the gigantic amplitude of the oscillations. As seen from Fig. 6a, a change of 1% in the external field changes the rate of the chemical reaction by 40 times, from 0.01 to 4 $\mu\text{g}/\text{cm}^2\text{min}$. In other words, since the rate 0.01 $\mu\text{g}/\text{cm}^2\text{min}$ lies within the limits of the measurement errors, a change of 1% in the external magnetic field, and of 0.1% in the sample induction in the state of magnetic saturation, leads practically to either a complete suppressed or a very intense chemical reaction. On the curve obtained at $T = 70^\circ\text{C}$, one can see clearly in the interval from 830 to 1170 Oe four large periods, in each of which there are five high-frequency oscillations, i.e., in the modulation interpretation, $\Delta H_1 = 17$ Oe and $\Delta H_2 = 85$ Oe. Thus, compared with

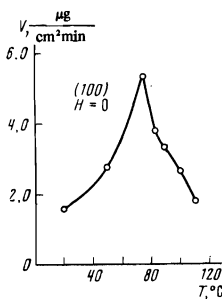


FIG. 5. Dependence of the nickel carbonylation reaction rate on the temperature in the absence of a magnetic field.

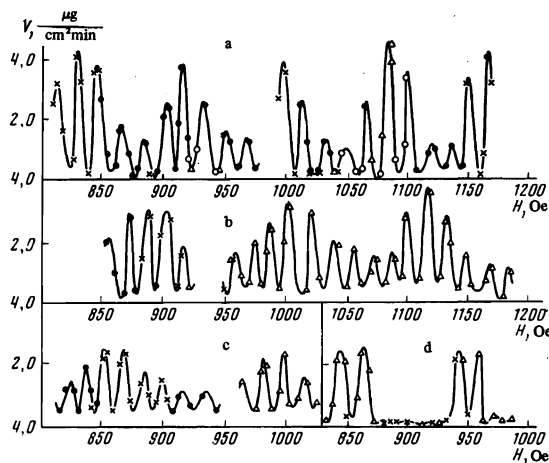


FIG. 6. Dependence of the oscillatory curves of the nickel carbonylation reaction rate on the temperature. Identical points on each curve represent uninterrupted measurement cycles. a) $T = 70^\circ\text{C}$, b) $T = 80^\circ\text{C}$, c) $T = 90^\circ\text{C}$, d) $T = 100^\circ\text{C}$.

room temperature, the period of the high-frequency oscillations remains practically unchanged, and for the low-frequency component the period has decreased by more than 2 times. If the beat hypothesis is used for the interpretation, we obtain $\Delta H_1 = 14$ Oe and $\Delta H_2 = 20$ Oe, i.e., the period of the first harmonic has decreased somewhat compared with room temperature, and that of the second harmonic has increased. The curves measured at $T = 80$ and 90°C have qualitatively the same form as at $T = 70^\circ\text{C}$, while at $T = 100^\circ\text{C}$ we obtain, as follows from Fig. 6d, a rather abrupt change in the character of the $V(H)$ curve, which calls naturally for an additional verification and study.

We proceed now to discuss the results. The only known physical mechanism that can be used to explain the observed oscillatory effects is, in our opinion, the quantization of the electron energy spectrum of the system in the magnetic field. This raises the two difficulties indicated above, namely the absence of periodicity in $1/B$ and the appearance of oscillations at room temperature.

We have already noted earlier^[1] certain hypothetical possibilities of getting around these difficulties. Disregarding these difficulties and taking into account the new experimental data presented above, let us attempt to see whether, with the contemporary information concerning the band structure of Ni, we can find a proper place for the observed quantum oscillations, i.e., a real Fermi-surface element with the appropriate experimental oscillatory characteristics. A good guideline for this can be the fundamental sinusoidal harmonic with $\Delta H = 40$ Oe, which is observed at $H \parallel [100]$. Using the well-known Lifshitz-Onsager quantization formula $S = 2\pi e/\hbar c \Delta(B^{-1})$ and the value $B = h + 4\pi I_S = 1000 + 6000 = 7000$ Oe, we obtain in k -space for the external Fermi-surface section area S , corresponding to the oscillation period $\Delta B = 40$ Oe, a value $S = 1.17 \times 10^{14}$ cm^{-2} , and a radius $k_F = 0.6 \times 10^7$ cm^{-1} for the circle with this area.

We see immediately that no Fermi-surface elements with such small extremal cross sections were observed by the usual methods of measuring oscillatory effects at helium temperatures. The minimum cross sections observed with the de Haas-van Alphen effect is the L-neck of the hyperboloid of revolution in the $[111]$ direc-

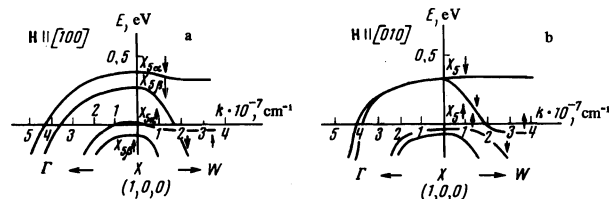


FIG. 7. Band structure of ferromagnetic nickel in the vicinity of the X point of the Brillouin zone. The bands X_2 and X_4 are not represented in the scheme.

tion with $S = 2.3 \times 10^{14} \text{ cm}^{-2}$, and the ellipsoidal hole pocket at the X point with extremal sections S that range from 8.7×10^{14} to $21.4 \times 10^{14} \text{ cm}^{-2}$ [5]. Furthermore, the change in the period of the oscillations corresponding to the L-neck, following rotation of H in the (100) plane, does not correspond at all to our experimental value. Consequently, a new Fermi-surface element must be sought, with parameters that are appropriate to our oscillations. Such a possibility is uncovered by the hypothesis that at room temperature there occurs, owing to the shifts of the sub-bands of the right-hand (\uparrow) and left-hand (\downarrow) spins, the new hole pocket at the $X_5\uparrow$ point proposed earlier [6] to explain one of the possible mechanisms of the orientational magneto-optical effect. At any rate, the parameters of this new hole pocket can agree fully with the required ones. Figure 7 shows a scheme explaining the considered variants. The parameters of the $X_5\uparrow$ pocket are reproduced in accordance with the aforementioned experimental data of Tsui [5] and the calculations of Zornberg [7] (the set IV of the band parameters). The placement of the $X_5\uparrow$ bands was in accordance with the hypothesis of [6] and the magneto-optical determinations of the proximity of the $X_5\uparrow$ level to the Fermi surface, which were carried out earlier [8] in such a way that the pocket dimension k_{XW} was equal to the value $k_F = 0.6 \times 10^7 \text{ cm}^{-1}$ obtained above. It is seen from the figure that the required transverse dimension of the pocket can be easily obtained via spin-orbit distortion of the shape of the band near the point $X_5\uparrow$ in the XW direction. The pure single-component character of the oscillations at $H \parallel [100]$ is attributed in this model to the existence of only one hole ellipsoid $X_5\uparrow$ in the [100] direction (see Fig. 7a), while the ellipsoids in the directions [010] and [001] do not come out from under the Fermi level (see Fig. 7b). Nor are any difficulties raised by the qualitative explanation of the anisotropy of the observed oscillations. For example, the decrease of the period of the fundamental harmonic on Fig. 3a, the decrease of the period of the fundamental harmonic on Fig. 3a, in comparison with Fig. 3b, can be attributed to an increase in the extremal cross section of the ellipsoid $X_5\uparrow$, located in the [100] direction, and the appearance of the low-frequency envelope of the component with a period on the order of 400 Oe can be attributed to the emergence of a hole ellipsoid $X_5\uparrow$, which is even several times smaller, in the [010] direction.

The two-component structure of the oscillation curve at $H \parallel [110]$ can be attributed, if the beat hypothesis is used, to the poor orientation of the single crystal and to the associated nonequivalence of the pockets $X_5\uparrow$ in the directions [100] and [010] (this assumption can be verified by adjusting the sample position and the fields by the zero-beat method). In the modulation interpretation, this can be attributed to the emergence of a small pocket $X_5\uparrow$ at $H \parallel [110]$ from under the Fermi

surface. This possibility exists in principle because, as shown by the Zornberg calculation [7], the spin-orbit components of the level $X_5\uparrow$ can behave in a rather unique manner—the decrease of the spin-orbit splitting of the components following the rotation of the vector I can proceed not via a symmetrical contraction of the components towards the center of gravity, but mainly via pulling of the lower component to the upper one (see, e.g., the calculations in [7] with the parameter set VII). Finally, the abrupt change in the form of the oscillation curve at $T = 100^\circ\text{C}$ (see Fig. 6) can be attributed to a transition from a closed ellipsoidal Fermi surface in the $X_5\uparrow$ band to an open one in the direction of the XW surface as a result of the upward temperature shift of the $X_5\uparrow$ band (i.e., the pocket vanishes, and with it the associated oscillations).

Let us dwell now on another variant of the explanation analogous to that given above. The point is that near the Fermi surface, at the point X, there can be also a d-type band $X_2\uparrow$ [7], and many of the arguments presented above can also be applied, in general outline, to the formation of hole pockets of the required dimension in the $X_2\downarrow$ band. This possibility must be kept in mind in principle. We have chosen a variant in which a hole pocket is produced in the $X_5\uparrow$ band for the following reasons: First, at helium temperatures, no hole pockets with such small dimensions has been observed at the X point, and the formation of the $X_5\uparrow$ pocket at room temperature can be attributed to a decrease in the exchange splitting of the X_5 band, which causes the upward motion of the $X_5\uparrow$ band. To the contrary, the $X_2\downarrow$ band should shift downward when the exchange splitting is decreased. Second, it is easy to visualize physically the sensitivity of the chemical reaction to the formation and quantization of hole pockets of the type $X_5\uparrow$ rather than $X_2\downarrow$. The point is that in the absence of these pockets in nickel there are no hole states of the d-type at all in the subband of the right-hand (\uparrow) spins, because the $X_5\uparrow$ level is the upper level of the d-subband of the right-hand spins. It is possible, of course, to assume that the chemical carbonylation reaction is also sensitive to the presence in nickel of hole d-orbitals of the X_2 type, and then preference must be given to the second variant of the explanation. We can summarize all the foregoing in the following manner: All that is well known concerning the nickel carbonylation reaction is that it begins with formation of a monomolecular chemisorbed CO layer on the surface of the nickel [9]. On the other hand, we do not know how the carbonyl molecule $\text{Ni}(\text{CO})_4$, which carries away in the gas phase one nickel atom from the surface, is produced in this layer. If we now assume that the probability of carbonyl formation depends on the number of the d-states of the $X_5\uparrow$ or $X_2\downarrow$ type at the Fermi level of the nickel, then it becomes possible in principle to explain the obtained experimental data in the manner indicated above.

The smallness of the produced pocket, and consequently, the smallness of the number of Landau levels, will perhaps help overcome the difficulty brought about by the absence of a periodicity in $1/B$, while the fact that the electron mean free path does not play any role in the rate of the chemical reaction will probably relax the requirements on the possibility of observing quantum oscillations at room temperature. At any rate, the results already obtained convince us of the need for further experimental and theoretical investigations of the observed so strong and characteristic influence of the magnetic field on the rate of the chemical reaction fol-

lowing so small a change in the field intensity.

We are sincerely grateful to V. V. Afanas'ev for help with the experiments.

¹G. S. Krinchik, R. A. Shvartsman, and A. Ya. Kapnis, *ZhETF Pis. Red.* **19**, 425 (1974) [*JETP Lett.* **19**, 321 (1974)].

²F. M. Rappoport and A. A. Il'inskaya, *Laboratornyye metody polucheniya chistikh gazov* (Laboratory Methods for Obtaining Pure Gases), Goskhimizdat (1963).

³V. F. Fikhtengol'ts and I. P. Kozlova, *Zavodskaya laboratoriya* **23**, 917 (1957).

⁴W. M. Goldberger, *Ind. Eng. Chem.*, **55**, 96 (1963).

⁵D. C. Tsui, *Phys. Rev.*, **164**, 669 (1967).

⁶G. S. Krinchik, *J. de Phys.*, **32**, C1, 1058 (1971).

⁷E. I. Zornberg, *Phys. Rev.*, **B1**, 244 (1970).

⁸G. S. Krinchik and E. A. Gan'shina, *Zh. Eksp. Teor. Fiz.* **65**, 1970 (1973) [*Sov. Phys.-JETP* **38**, 983 (1974)].

⁹L. H. Little, *Infrared Spectra of Absorbed Species*, Academic, 1967.

Translated by J. G. Adashko.

246